Atmos. Chem. Phys. Discuss., 15, C1488–C1496, 2015
www.atmos-chem-phys-discuss.net/15/C1488/2015/

Atmospheric Chemistry and Physics Discussions

Interactive comment on "Investigating the frequency and trends in global above-cloud aerosol characteristics with CALIOP and OMI" *by* R. Alfaro-Contreras et al.

H. Jethva

hiren.t.jethva@nasa.gov

Received and published: 10 April 2015

The submitted manuscript examines the multi-year variations, which has been referred to as 'trend analysis' in the paper, of the above-cloud aerosols (ACA) detected by two different sensors and techniques, i.e., one based on the space lidar CALIOP on board CALIPSO satellite, and one that relies on the columnar cloud and aerosol parameters measured from MODIS and OMI passive imagers. Author carries out ACA detection analysis on a global scale with emphasis on several aerosol laden regions and found discrepancies between the two techniques. Of the several interesting issues discussed in the manuscript and also raised by the anonymous reviewers, the trend in ACA fre-

quency detected using OMI-MODIS technique drew my attention most.

Since mid-2007, OMI observations have been affected by a likely external obstruction that perturbs both the measured solar flux and Earth radiance. This obstruction affecting the quality of radiance at all wavelengths for a particular viewing direction is referred to as "row anomaly" since the viewing geometry is associated with the row numbers on the charge-coupled device detectors. The row anomaly issue was detected first time in mid-2007 for few rows which over the period of operation expanded to other rows in 2008 and later. Figure 1 shows the current status of the row anomaly as identified by the OMI group at NASA Goddard. At present, about half of the total 60 rows across the track are identified and flagged as row anomaly affected positions for which no physical retrievals are being performed.

Given the fact that OMI has lost its viewing capability by half post 2008 period, which has directly affected the frequency of measurements globally over both clear and cloudy skies, the 'all-sky' frequency of measurements of aerosol and cloud parameters should go down. However, we learn from the Figure 8 of the submitted paper that author adopts the 'cloudy-sky' as reference measurements in order to calculate the freq. of occurrence of ACA from both CALIOP and OMI sensors. Author attributes the apparent trend in OMI-derived ACA freq. to the observed dependence of UV-AI on the geometry. First, we verified this dependence by plotting the UV-AI as a function of row # for data collected during 2007.

Figure 2 shows the 2007 (prior to the 2008 onset of the row anomaly) annual average AI parameter as a function of scan viewing position (or satellite zenith angle, nadir corresponds approximately to position 30) for cloudy scenes (LER > 0.25). A scan angle dependence likely associated with cloud scattering phase function effects is observed. The resulting AI values are lowest in the vicinity of nadir, and larger at the far off-nadir positions on both ends of the scan, but largest on the extreme positions on the right side. As a consequence of the row anomaly the observing capability associated positions 24 to 54 has been lost. Since the set of lost viewing conditions contain the lowest

range of AI values for high LER conditions, after the anomaly onset the relative frequency of occurrence of aerosol events with AI larger than a given threshold value will be larger than during the pre-anomaly conditions, which seems qualitatively consistent with the reported finding. We conducted an analysis similar to one presented in the manuscript to verify the OMI ACA frequency results obtained by the author.

First, we follow the same definition for calculating the freq. of ACA as adopted in the manuscript which is based on the 'cloudy-sky' measurements. The freq. of ACA is defined as,

Freq.ACA=(Number of days with ACA condition)/(Number of cloud-sky days in a month)

As suggested by the anonymous reviewers, author should properly define the ACA freq. in the manuscript which is currently missing. Secondly, the conditions or satellite measurements for detecting ACA should be determined in an appropriate way. Given the fundamental difference between signal that is measured by CALIOP (back-scatter) and OMI (aerosol absorption), these conditions would be different for both sensors. In our paper by Torres et al. [2012] which introduced a novel approach to retrieve AOD above cloud and aerosol-corrected COD simultaneously using OMI observations, we have shown that the UV-AI and Lambertian Equivalent Reflectivity (LER) measured by OMI can adequately identify the presence of absorbing aerosols above cloud. While UV-AI (>1.0) serves as a strong indicator of absorbing aerosols, the LER (>0.25) can be a measure of the brightness of background, in this case its cloud deck. These thresholds in UV-AI and LER were determined based on the radiative transfer calculations and co-located OMI and MODIS cloud products.

Using above thresholds as a benchmark for detecting ACA, we calculate the freq. of ACA for each 0.25 x 0.25 degree grid box globally for each month starting from Jan 2005 through Dec 2014. Then, a linear trend has been calculated using monthly freq. of ACA estimated in the previous step. Figure 3 shows multi-year variations in the monthly ACA frequency for three datasets, i.e., 'Alldata' where all the OMI data with

UV-AI>1.0 and LER388>0.25 were used, 'FilteredData' where measurements for some specific geometries were excluded from 'AllData', and 'FilteredDataRow1to23' in which only first 23 rows of OMI were used in the calculations.

Further analysis of the OMI data over the regions of strong positive trend, particularly for latitudes greater than 70 deg. revealed that these observations are associated with a set of specific geometry which gave rise to the magnitudes of UV-AI (>1.0 & <2.0) in the cloudy situations. These geometries are:

Solar zenith angle > 60 deg. & Viewing zenith angle >60 deg.

OR

Scattering Angle <100 deg.

Note that the OMI UV-AI has been calculated following a Lambertian approach which appears to break down for the cloudy pixels observed under the combination of above geometries. We believe that the reason for the non-validity of Lambertian assumption under these conditions could be the phase function of clouds which is likely being not treated adequately at above geometries. The deviation of the Lambertian assumption from the true cloud phase function, therefore, can result in higher UV-AI (>1.0) which subsequently interpreted as aerosols above cloud in the present analysis. It is, therefore, essential to 'filter' the OMI data by excluding above geometries from the analysis in order to better understand trend or inter-annual variation of freq. of ACA. As a result of filtering out the non-aerosol related signal, the monthly freq. of ACA has reduced significantly from the non-filtered dataset. Nevertheless, both datasets reveal a positive trend in ACA freq. which concurs with the results reported in Figure 8 of the submitted manuscript.

Knowing the fact that UV-AI exhibits scan angle dependence and since OMI encountered the row anomaly beginning 2009, use of full 60 row positions during pre-anomaly period and 23 positions during post-anomaly period can likely result in an 'apparent'

trend in the frequency of detection of aerosol episodes using OMI data based on a fixed AI threshold. Particularly, this is true for the ACA situation for which use of first 23 clean rows after 2008 associated with larger viewing zenith angle and hence larger UV-AI yields an increase in cloud-sky ACA frequency relative to the pre-anomaly period. In order to derive a meaningful trend from OMI, therefore, one should look at the measurements acquired by first 23 rows over the entire mission. These rows (1 through 23) were almost unaffected by the row anomaly throughout OMI mission, and therefore can provide a consistent and unbiased record of measurements for the trend analysis.

The 'green' color coded data points in Figure 3 represent the monthly variations in ACA frequency derived using Row # 1 through 23 throughout the OMI decadal record. On contrary to the results obtained in previous two cases, ACA frequency derived from OMI Row # 1 through 23 shows almost no trend which is very much consistent with the results obtained using CALIOP data. This is because the measurements acquired by Row # 1 through 23 have nearly same viewing zenith angle for each respective row, and thus use of these clean rows eliminate scan angle related bias in the decadal trend analysis.

Suggestions to author: The analysis presented in our report reveals that the trend in ACA derived from OMI observations depend on how we identify ACA situation and what dataset is being used for the analysis. We strongly recommend author to redo OMI analysis using measurements from Row # 1 through 23 and the data filtering scheme suggested above. The only difference then will be the cloud mask for which we used OMI LER observations, whereas author uses MODIS cloud product. We expect a marginal difference in the results due to the different cloud schemes. Since aerosols above clouds is a regional phenomenon, it is desirable to carry out trend analysis separately for the regions where ACA situation is frequently observed from satellites, i.e., south-east Atlantic Ocean, tropical Atlantic Ocean-off the coast of western Sahara, south-east and north-east Asia, and northern Arabian Sea.

Hiren Jethva & Omar Torres OMI Aerosol Group NASA Goddard Space Flight Center Greenbelt, MD 20771 USA

Interactive comment on Atmos. Chem. Phys. Discuss., 15, 4173, 2015.

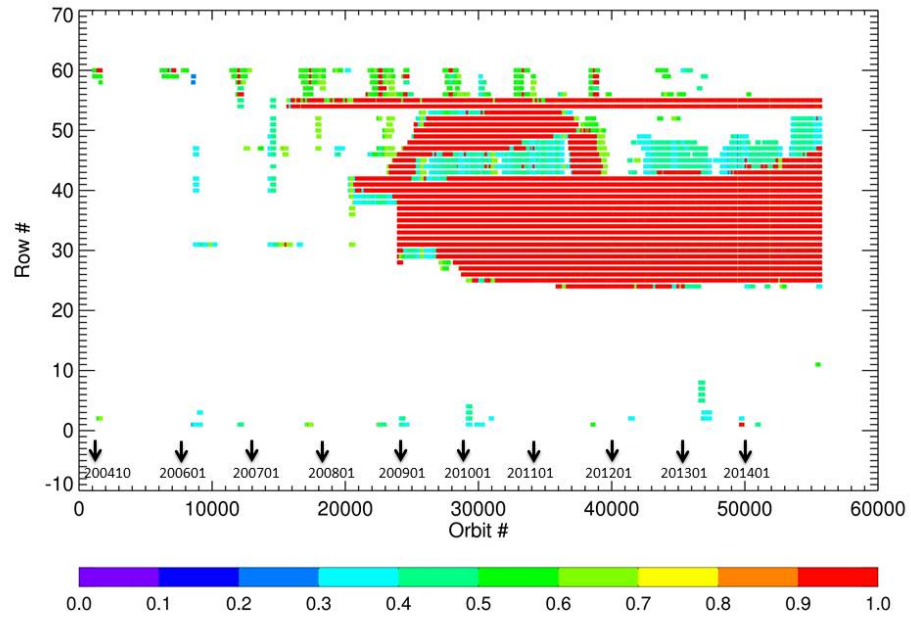

Fig. 1. OMI row anomaly status as of March 2015 as used by OMI group at NASA Goddard. The color scale indicates portion of the orbit that is affected by the row anomaly.

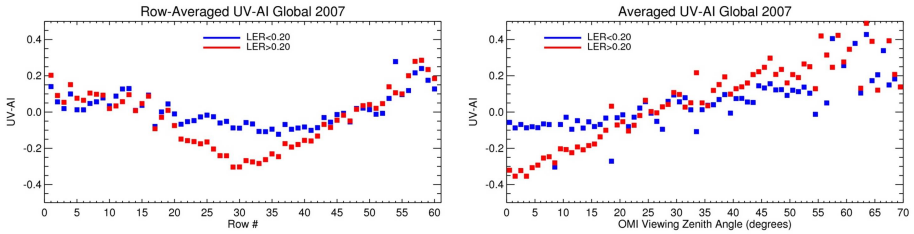

Fig. 2. OMI UV Aerosol Index as a function of Row number (left) and satellite viewing zenith angle (right) for year 2007. All OMI UV-AI data collected by repsective rows and for a given viewing zenith angle b

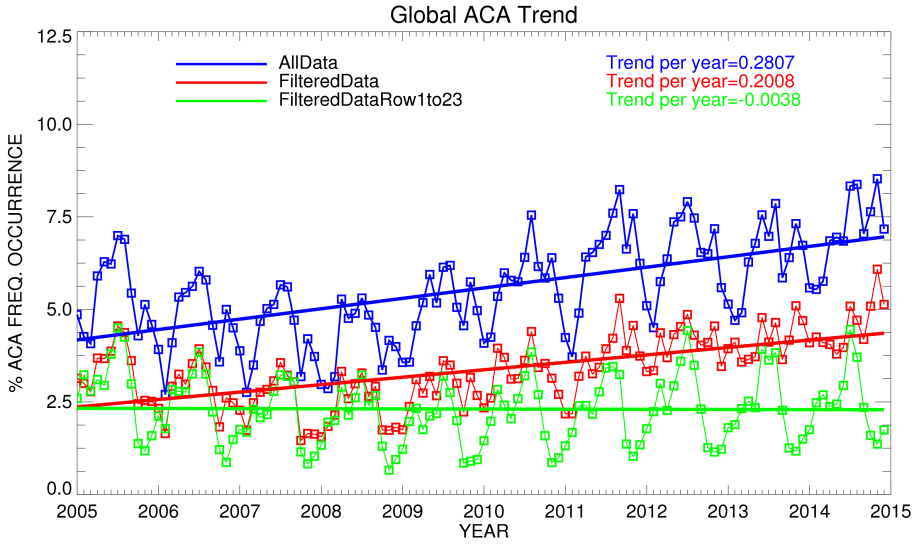

Fig. 3. Multi-year variations of the global ACA frequency of occurrence for unfiltered and filtered OMI data. Refer to text for the three types of datasets.